Review of structures in low-energy bremsstrahlung: classical and quantum descriptions

O. I. Obolensky[a,b]‡, **R. H. Pratt**[b]

[a] *A. F. Ioffe Physical-Technical Institute, St. Petersburg 194021, Russia*
[b] *University of Pittsburgh, Pittsburgh, PA 15260, USA*

Abstract. A brief review of recent advances in studying structures in energy dependence of the bremsstrahlung cross sections for low incident electron energies is presented. Examples of structures are given in both classical and quantum formalisms. It is shown that the origin of the structures can be formulated as a lack of contribution to the radiation from electrons with certain angular momenta at certain energies. In quantum mechanics the lack of contribution to the total cross section from certain electron angular momenta is due to zeroes in corresponding dipole matrix elements. In classical mechanics summation over angular momentum is replaced by integration and structures are due to suppressed or enhanced contribution from certain intervals of angular momentum. A survey of the known properties of the matrix elements zeroes is given.

1. Introduction

We give a brief review of recent advances in low-energy electron bremsstrahlung. We mainly focus on the structures which appear in the dependences of the differential bremsstrahlung cross section and the radiation asymmetry parameter on the incident electron energy. These structures seem to be a characteristic of the low incident electron energy region (for example, below 200 eV for Al).

The structures were initially discovered [1] within the classical formalism [2,3] in the asymmetry parameter of radiation (see definition in section 2) considered as a function of electron energy T for fixed various ratios of photon energy k/T. Later the structures were identified in the differential cross section $k\mathrm{d}\sigma/\mathrm{d}k$ [4]. Later similar structures have also been observed in the quantum case within the partial waves formalism, at approximately the same energies as the classical structures [5, 6].

Structures are observed both in quantum mechanical and classical descriptions of bremsstrahlung. In both approaches they may be understood as resulting from lack of contribution to the radiation from electrons with certain angular momenta at certain energies. In quantum mechanics this means that the some of the dominant partial contributions to the total cross section vanish for certain dipole transitions at certain combinations of initial and final electron energies due to zeroes in the corresponding

‡ Corresponding author. *E-mail address:* oleg@stribor.phyast.pitt.edu

dipole matrix elements. In classical mechanics summation over the angular momenta is replaced with integration; nevertheless, it is possible to isolate intervals of the angular momenta whose contribution to the cross section is suppresed at certain electron energies.

Currently, there are no experimental results for the electron energy range where the structures are expected to be found. There are, however, recent experiments studying energy dependence of bremsstrahlung (at fixed photon energy) for somewhat larger energies for Ar targets [7, 8].

Zeroes in radial matrix elements, which give rise to the structures under discussion, are a general phenomena occuring in various circumstances and leading to structures in various observables. They exist both in relativistic and non-relativistic domains. Most frequently they are found in numerical calculations and often only a very general explanation can be given. Only in exceptional cases have properties of the zeroes been established analytically. For example, one can rigorously prove that relativistic bound-free dipole matrix elements vanish at certain energies, for any scattering potential [9]. For relativistic quadrupole transitions zeroes do also exist but no rigorous analytical description of their properties has been given yet [9].

Probably, the best known example of structures caused by matrix elements zeroes is Cooper minima in photoeffect cross sections. These minima are due to zeroes in bound-free dipole matrix elements. These zeroes have been thoroughly studied and tabulated [10–13].

We have found that zeroes in free-free dipole matrix elements are also of a general nature. Our data suggest that they occur for at least some of the dipole transitions in the field of any neutral atom, starting from Lithium. The typical range of incident electron energies at which zeroes occur is 1-100 eV.

It should be noted that the results presented in the review concern the so-called ordinary bremsstrahlung, resulting from the acceleration of a charged particle in the static field of a target. There is also another mechanism of bremsstrahlung, the so-called polarizational bremsstrahlung, resulting from dynamic excitation (polarization) of a target's structure by a projectile. For a discussion of these two mechanisms see [14], or more detailed reviews in [15–18]. As with ordinary bremsstrahlung, polarizational bremsstrahlung may also be discussed from a classical viewpoint, as in [19] or more recently in [20]. A more complete treatment should also include this second mechanism of bremsstrahlung production. However, the structures in the energy dependence discussed here are pronounced even in the case of very low photon energies, where dynamic polarization of the target is negligible. For small photon energies polarization of the target is static in nature and can be accounted for by adding a polarizational "tail" to the atomic potential thereby redefining the ordinary bremsstrahlung component. Preliminary calculations show that this does not change the overall behaviour of the structures [21] and, therefore, the polarizational mechanism can be left out in the initial stage of exploration of the structures.

The atomic system of units $\hbar = e = m = 1$ is used throughout the paper.

2. Quantum bremsstrahlung

It is known that the Born approximation for bremsstrahlung calculations is not adequate for the case of slow electrons and one needs to use the partial waves expansion of the incident electron wave functions (the so called distorted partial wave approximation) [22–25]. In this approach the total bremsstrahlung cross section is expressed as a sum of partial contributions each of which corresponds to a dipole transition between the electronic partial waves:

$$k\frac{\mathrm{d}\sigma}{\mathrm{d}k} = \frac{16\pi^2}{3}\frac{k^4}{T_1 c^3}\sum_{\ell_1=0}^{\infty}\sum_{\ell_2=\ell_1\pm1}\ell_>|\mathcal{M}_{\ell_1,\ell_2}(T_1,T_2)|^2. \tag{1}$$

Here indexes '1' and '2' refer to initial and final state of the incident elecron, respectively, k is the photon energy, T is the electron energy, ℓ is the angular momentum, $\ell_> = \max(\ell_1,\ell_2)$, c is the speed of light, $\mathcal{M}_{\ell_1,\ell_2}(T_1,T_2)$ is the radial dipole matrix element between the states $|T_1,\ell_1>$ and $<T_2,\ell_2|$,

$$\mathcal{M}_{\ell_1,\ell_2}(T_1,T_2) = \int_0^\infty P_{E_2,\ell_2}(r) r P_{E_1,\ell_1}(r)\mathrm{d}r, \tag{2}$$

where $P(r)$ are the radial wave functions normalized to the δ-function of energy.

For low electron energies in scattering from neutral atoms only first few terms contribute to the sum in equation (1). Hence, the total cross section is very sensitive to the possible structures in the dominant matrix elements. In particular, if a dominant matrix element vanishes at some certain ratio of initial and final electron energies, the square of the matrix element as a function of one of the energies has a sharp minimum, reaching zero, which can be of the form $\sim (E - E_{\min})^2$.

We illustrate the consequences of the zeroes in the dominant matrix elements in Figure 1, where the energy dependence of the total bremsstrahlung cross section is plotted for three choices of the fraction of incident electron energy which is radiated. The origin of the wide smooth minimum at an incident electron energy of about 10 eV is made clear in Figure 2, where the partial contributions to the sum (1) are presented for two ratios of the photon and electron energies. The figure makes it evident that the structures seen in the energy dependence of the total cross section are to be understood as resulting from zeroes in the dominant matrix elements, namely, in the transitions $0 \leftrightarrow 1$ and $1 \leftrightarrow 2$ in this particular case. Note that in the soft photon limit, $k/T \to 0$, matrix elements $0 \to 1$ and $1 \to 0$, $1 \to 2$ and $2 \to 1$, etc. are equal, while for larger k/T the behaviours of the pairs of matrix elements are more spread out, resulting in a slight widening of the structures in the total cross section.

Angular distributions of radiation are even more sensitive to zeroes in dominant matrix elements. For dipole radiation it is customary to express the doubly differential cross section describing the radiation emitted into a solid angle $\mathrm{d}\Omega_k$, in the frequency interval $k, k + \mathrm{d}k$, in terms of the singly differential cross section $k\mathrm{d}\sigma/\mathrm{d}k$ and the asymmetry parameter of radiation a_2:

$$k\frac{\mathrm{d}^2\sigma}{\mathrm{d}\Omega_k \mathrm{d}k} = \frac{1}{4\pi}k\frac{\mathrm{d}\sigma}{\mathrm{d}k}\left(1 + \frac{a_2(k)}{2}P_2(\cos\theta_k)\right). \tag{3}$$

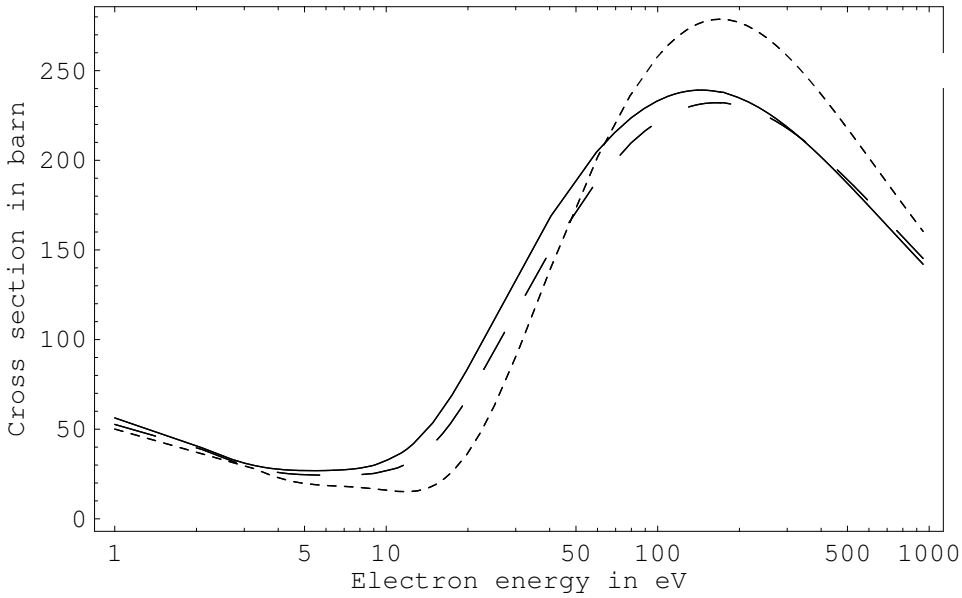

Figure 1. Energy dependence of the bremsstrahlung cross section (1), for Al for different ratios of photon energy k and incident electron energy T: solid line $k/T = 0.01$, dashed line $k/T = 0.2$, dotted line $k/T = 0.6$. The figure is taken from [5].

Here P_2 is the Legendre polynomial of second order and θ_k is the azimuthal angle of emission of the photon.

The asymmetry parameter of radiation is the single system-specific parameter defining the angular distribution of radiation. The dependence of the asymmetry parameter on the incident electron energy contains even more pronounced structures than the spectra, which are again due to the zeroes in the dominant matrix elements. An example of such structures for Al is presented in Figure 3.

A remarkable fact is that the character of the structures (it is especially true for the spectra and in a lesser degree for the angular distributions) is largely independent of the ratio k/T, and it is well characterized by the soft photon limit $k/T \to 0$. Anticipating, we can add that this is also the case for the classical description of the bremsstrahlung process. In the classical approach this result is explained as being due to the fact that the major part of radiation is emitted near the point of maximum acceleration, i.e. in the vicinity of the turning point of the classical trajectory. At that point the electron kinetic energy is much larger that the initial electron energy, and therefore it is much larger than all physically allowed energies of radiation [19].

We may expect that the structures arising due to zeroes in the dominant matrix elements can also be observed in bremsstrahlung spectra (1). The structures would appear in spectra for certain incident electron energies, while there will be no structures

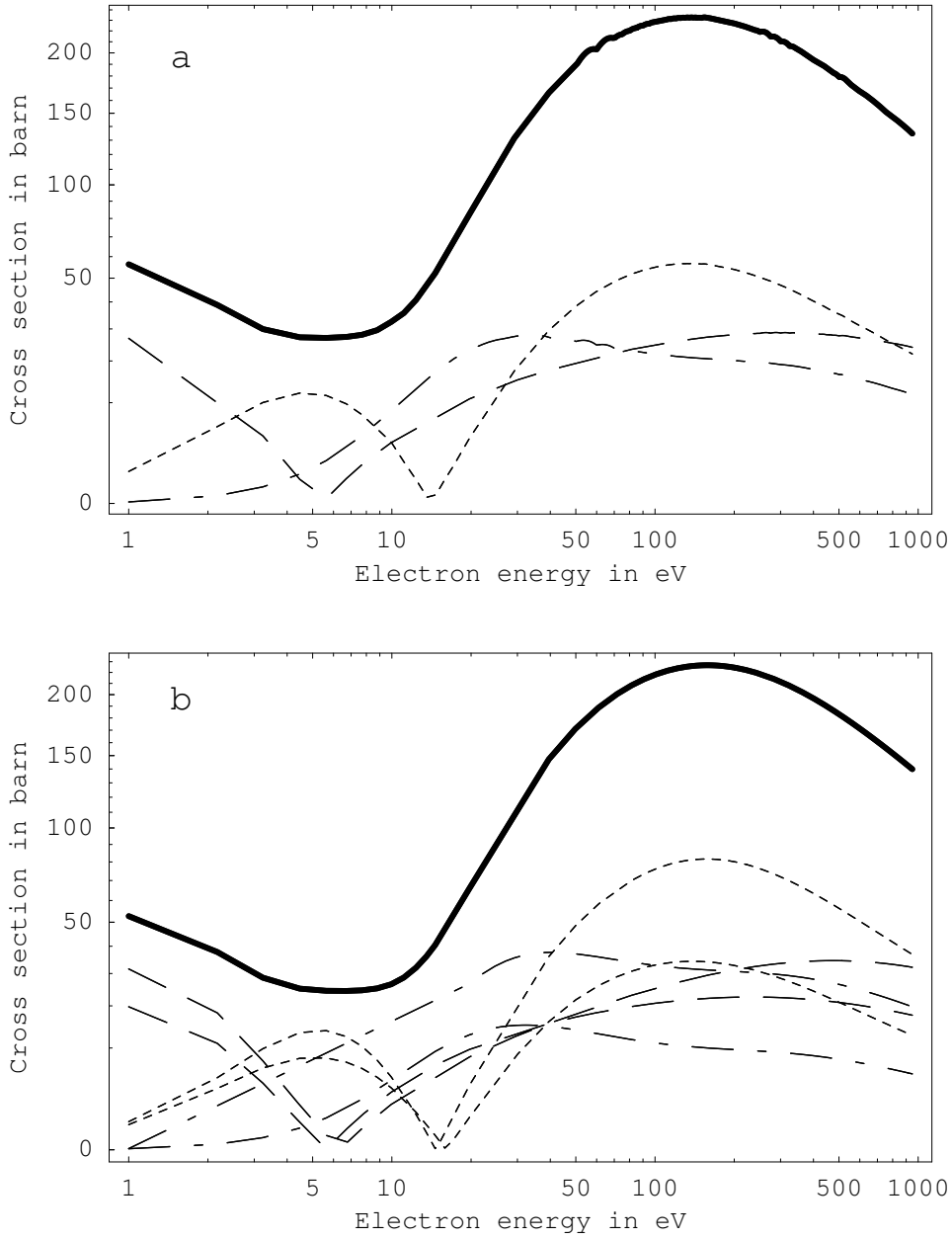

Figure 2. Partial contributions of dominant matrix elements to the total bremsstrahlung cross section (thick solid line) for the two values of ratio k/T: 0.01 (a) and 0.2 (b). Dashed lines correspond to $0 \to 1$ and $1 \to 0$ transitions, dotted lines correspond to $1 \to 2$ and $2 \to 1$ transitions and dashed-dotted lines correspond to $2 \to 3$ and $3 \to 2$ transitions. Note that for the soft photon limit $k/T \to 0$ matrix elements $\ell \to \ell'$ and $\ell' \to \ell$ are equal. For finite values of k/T the matrix elements are spread out; we do not label them separately here. The figure is taken from [5].

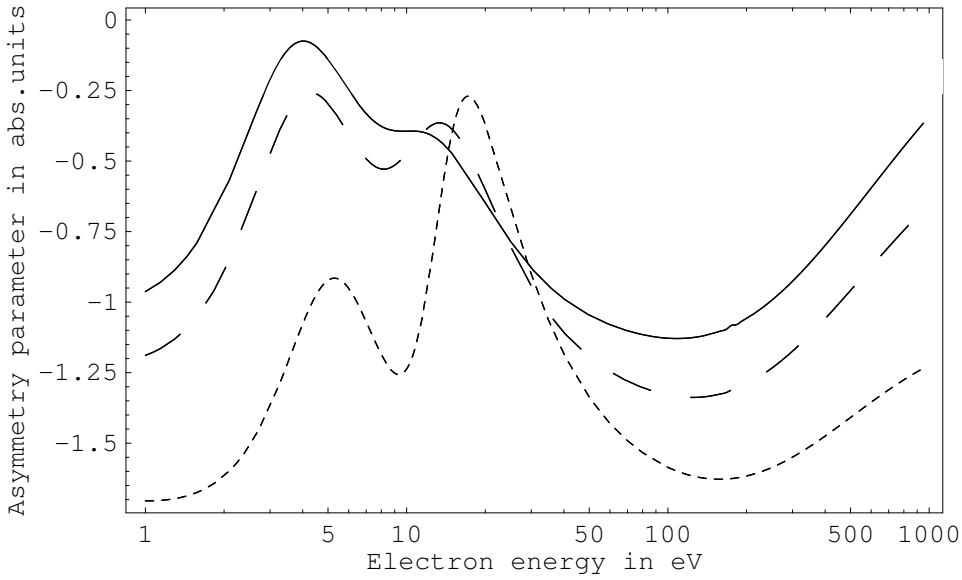

Figure 3. Energy dependence of the asymmetry parameter a_2, for Al for different ratios of photon energy k and projectile electron energy T: solid line $k/T = 0.01$, dashed line $k/T = 0.2$, dotted line $k/T = 0.6$. The figure is taken from [5].

at other energies. To predict electron and photon energies at which the structures are expected to appear one needs to understand the properties of the matrix element zeroes.

3. Zeroes of dipole matrix elements

3.1. Trajectories of matrix element zeroes

To study properties of matrix elements and in particular properties of their zeroes, it is convenient to consider the matrix element for every given pair of angular momenta ℓ_1 and $\ell_2 = \ell_1 \pm 1$ as a function of two variables – initial and final electron energies T_1 and T_2. Then every free-free transition (both T_1 and T_2 are positive for bremsstrahlung and inverse bremsstrahlung) corresponds to a point in the first quadrant of the (T_1, T_2) plane. The matrix element is a continuous function of T_1 and T_2 over the first quadrant of the (T_1, T_2) plane (except for the diagonal $T_1 = T_2$) and can be presented as a surface in 3D space. On the diagonal, i.e. in the soft photon limit, $T_1 = T_2$, the matrix element diverges as $1/(T_1 - T_2)^2$.

To smooth out the behaviour of the matrix element near the soft photon limit $T_2 \to T_1$, one can use the acceleration form of the matrix element:

$$\mathcal{M}_{\ell_1,\ell_2}(T_1, T_2) = -\frac{4}{(T_1 - T_2)^2}\mathcal{M}^{(\mathrm{a})}_{\ell_1,\ell_2}(T_1, T_2), \tag{4}$$

$$\mathcal{M}^{(\mathrm{a})}_{\ell_1,\ell_2}(T_1, T_2) = \int_0^\infty P_{E_2,\ell_2}(r)\frac{\mathrm{d}V(r)}{\mathrm{d}r}P_{E_1,\ell_1}(r)\mathrm{d}r. \tag{5}$$

Here $V(r)$ is the atomic potential. Equality (4) holds for $T_1 \neq T_2$, when the "surface" terms which generally appear in relations between different forms of the matrix element

vanish (if the acceleration form is adopted for the entire integration interval). In the case $T_1 = T_2$, there are additional singular terms, containing the Dirac's delta-function $\delta(T_1 - T_2)$ and its derivatives, on the right hand side of equation (4) [26–29].

For further simplification of the matrix element behaviour in the (T_1, T_2) plane, it is convenient to re-normalize the wave functions as

$$P(r) \cong r^{\ell+1} \quad \text{for } r \to 0. \tag{6}$$

The boundary condition (6) does not depend on energy, so that it can be applied to normalize any solution of the Schrödinger equation, including bound, unbound§, continuum states, and states with complex energies. The matrix elements calculated with these functions are called reduced matrix elements, because (6) omits the common normalization factors which do not have the simple analytical properties in energy of (6). We denote the reduced matrix element as $\overline{\mathcal{M}}$. We note that the renormalization does not change any properties of the matrix elements zeroes, it just makes the surface of the matrix element as a function plotted over the first quadrant of the (T_1, T_2) plane smoother.

We plot an example of a matrix element surface in Figure 4 for the reduced matrix element for the case of a $d \to p$ transition in the field of neutral Ba. The intersection of the matrix element surface with the (T_1, T_2) plane is a trajectory on which the matrix element is zero.

The thus obtained trajectories of matrix elements zeroes are much more convenient object of study. Below we list some of the regularities found in the behavior of such trajectories [30]. Understanding the general behavior of the trajectories as a function of degree of ionicity, angular momentum, and features of the atomic potential is useful for better understanding the general properties of radiation matrix elements and for predicting the structures in the bremsstrahlung cross sections.

- Our sampling over the range of Z (and theoretical considerations discussed in the next subsection) suggest that zeroes are observed in at least some matrix elements for all elements, starting from $Z > 2$.
- In electron bremsstrahlung from neutral atoms zeroes in dipole matrix elements are observed in all transitions involving either an initial or a final electron state with an angular momentum for which there is at least one bound state in the neutral atom potential. For example, zeroes occur in $s \to p$ and $p \to d$ transitions for Na (for which s and p states can be bound) and in $s \to p$, $p \to d$ and $d \to f$ transitions for Ba (for which s, p, and d states can be bound).
- There is a general pattern of evolution for the trajectories of zeroes with increase of ionicity:

§ An unbound state is a state with a negative energy which is not an eigenvalue of the Schrödinger equation; the wave function of such a state is divergent at infinity. However, if the energy of an unbound state is less than the energy of a bound state (in absolute value), than the integrand in (2) is finite at infinity and the integral converges.

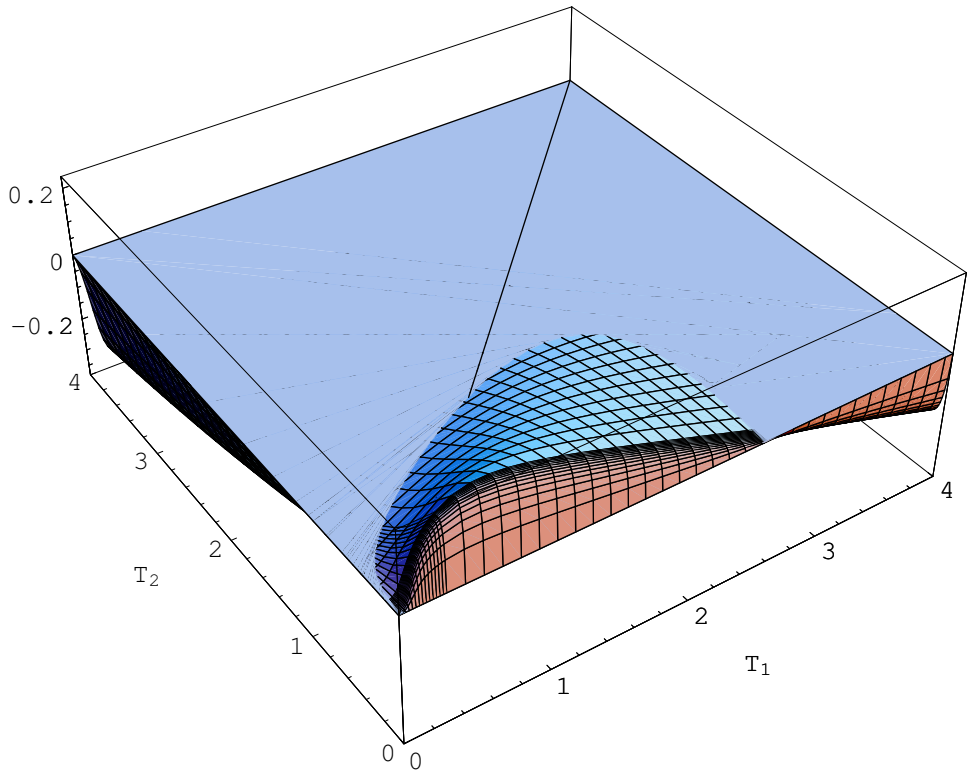

Figure 4. The reduced matrix element for a $d \to p$ transition for Ba as a function of initial and final electron energies. The intersection of the surface with the (T_1, T_2) plane is a trajectory on which the matrix element is equal to zero. The figure is taken from [6].

– For neutral atoms the trajectories always cross the diagonal (where initial and final energies of the electron coincide, $T_1 = T_2$). In terms of consequences for physical processes this means that zeroes in the matrix element occur for both up and down transitions, $\ell_1 \to \ell_2$ and $\ell_2 \to \ell_1$.
– With increasing ionicity the trajectories shrink towards the origin, still crossing the diagonal for low degrees of ionicity, but ceasing to cross the diagonal for higher degrees of ionicity, see Figure 5. In the latter case the trajectories approach and follow the diagonal towards the origin not crossing it. The degree of ionicity at which the trajectories cease to cross the diagonal depends on transition and element number. For lighter elements there are situations when even for singly ionized atoms there is no diagonal crossing by the trajectory.
– If a trajectory does not cross the diagonal, it therefore stays either completely above or completely below the diagonal, and energy conservation law implies that zeroes in matrix element can occur for only one direction of the transition (up or down). Our calculations show that the trajectories stay closer to the axis with higher angular momentum. This leads us to the conclusion that for the considered ionicity range zeroes in matrix elements can occur for transitions "down" for the case of emission of radiation (bremsstrahlung) and

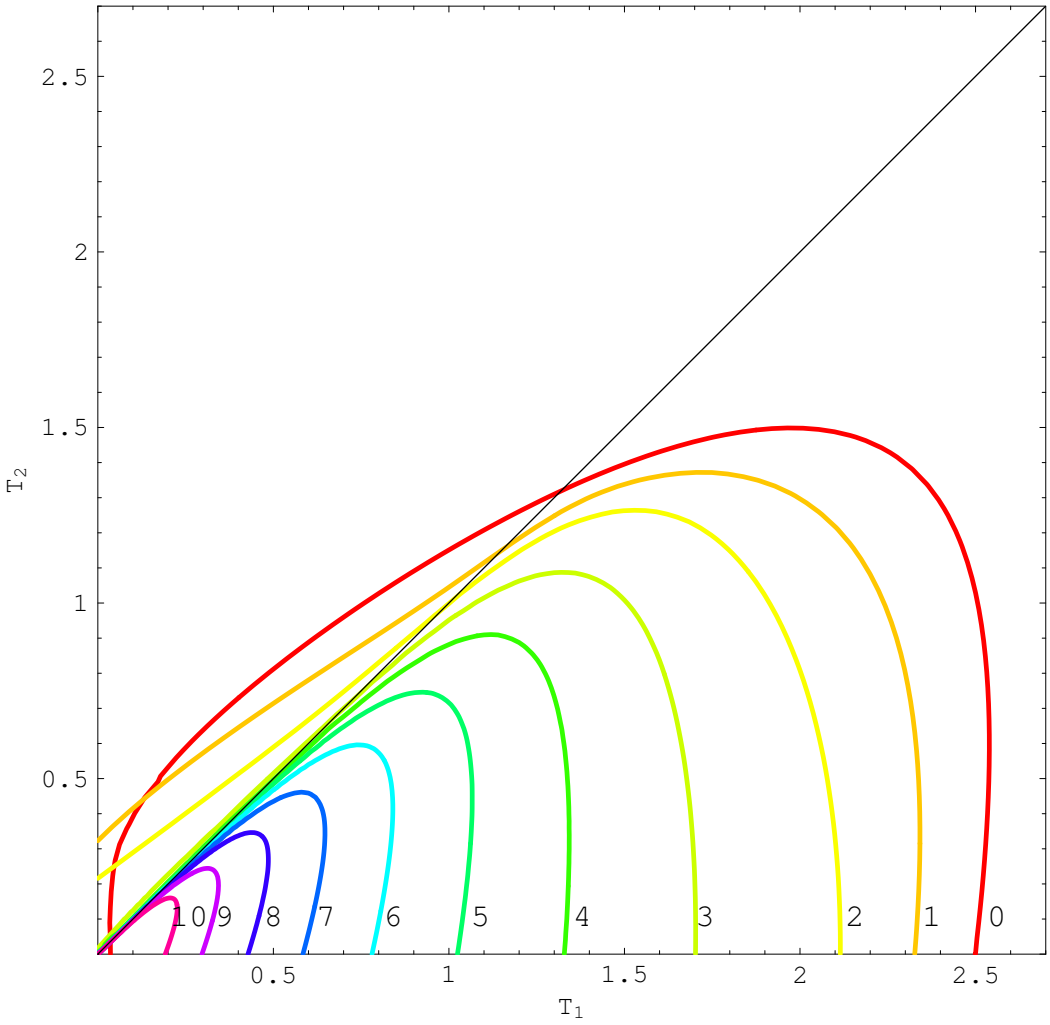

Figure 5. Evolution with ionicity of the trajectories of dipole matrix element zeroes for neutral and partly ionized Ba, for a $d \to p$ transition. Numbers on the plot denote the degree of ionicity for each trajectory. The figure is taken from [30].

for transitions "up" for absorption of radiation (inverse bremsstrahlung).

  - Eventually, for high enough ionicity, trajectories disappear from the free-free quadrant, in accord with the analytical result predicting that there are no zeroes in the point Coulomb field [31, 32]. Trajectories survive for higher degrees of ionicity for higher angular momentum (i.e. with increasing ionicity the $s \to p$ trajectory disappears first, then $p \to d$, etc.).

- For a given ionicity, the larger the angular momenta involved, the further the trajectory is away from the origin (i.e. zeroes occur at larger energies for higher angular momenta).

In the next subsection we will indicate how the properties of the atomic potential can be used for predicting at least some of the features in the behaviour of the trajectories.

3.2. Properties of atomic potential and matrix elements zeroes

A general remark is that both bound-free and free-free dipole matrix elements can be studied for screened atomic and ionic potentials only. The screened nature of the potentials in which the transitions take place is the crucial condition for existence of zeroes, since there is a theorem which states that there are no zeroes in dipole matrix elements for point Coulomb potentials [31, 32].

It appears that many of the properties of the trajectories of dipole matrix elements zeroes can be explained in terms of the properties of short range phaseshifts in a given potential. It is known that when $T_2 \to T_1$ (the soft photon limit) the reduced dipole matrix element is determined by the difference of the short range phaseshifts δ_1 and δ_2 for the corresponding angular momenta ℓ_1 and ℓ_2 [33]:

$$\mathcal{M}_{\ell_1,\ell_2}(T_1, T_2) \to \frac{4\sqrt{T_1}}{\pi} \sin(\delta_1 - \delta_2). \tag{7}$$

Therefore, at every energy T for which the phaseshift difference between ℓ_1 - and ℓ_2 -waves is equal to an integral multiple of π, the dipole matrix element has a zero. This means that the trajectory of zeroes crosses the diagonal in the (T_1, T_2) plane at this energy T.

Levinson's theorem [34–36] connects a phaseshift at zero energy $\delta_\ell(0)$ to the number of bound states n_ℓ with given angular momentum ℓ in a given neutral potential: $\delta_\ell(0) = n_\ell \pi$. Knowing the initial difference of the phaseshifts and recalling that phaseshifts tend to zero as $T \to \infty$, one may predict that the minimum number of diagonal crossings is

$$N_{\min} = n_1 - n_2 - 1, \tag{8}$$

where n_1, n_2 are the numbers of bound states with angular momenta ℓ_1 and ℓ_2, with $\ell_1 < \ell_2$.

For example, the potential of neutral Ne binds two s -states and no p -states ($n_s = 2$, $n_p = 0$), requiring at least one diagonal crossing of a trajectory of zeroes. In Figure 6 we show the dependence of the phaseshifts for s- and p-waves for neutral Ne. The vertical arrow shows the momentum p for which the difference between the two phaseshifts equals π. At this momentum the trajectory of the zero crosses the diagonal.

A similar argument can be made for ionic potentials, where the phaseshifts due to the short range part of the ionic potential can be connected to the quantum defect $\mu(n)$, defined by fitting the n^{th} energy level

$$E_n = -\frac{Ry}{(n - \mu(n))^2}, \tag{9}$$

where Ry is the scaled Rydberg constant. Then [35, 36]

$$\delta(0) = \mu(\infty)\, \pi \tag{10}$$

and

$$N_{\min} = \left[\frac{\mu_1 - \mu_2}{\pi}\right]. \tag{11}$$

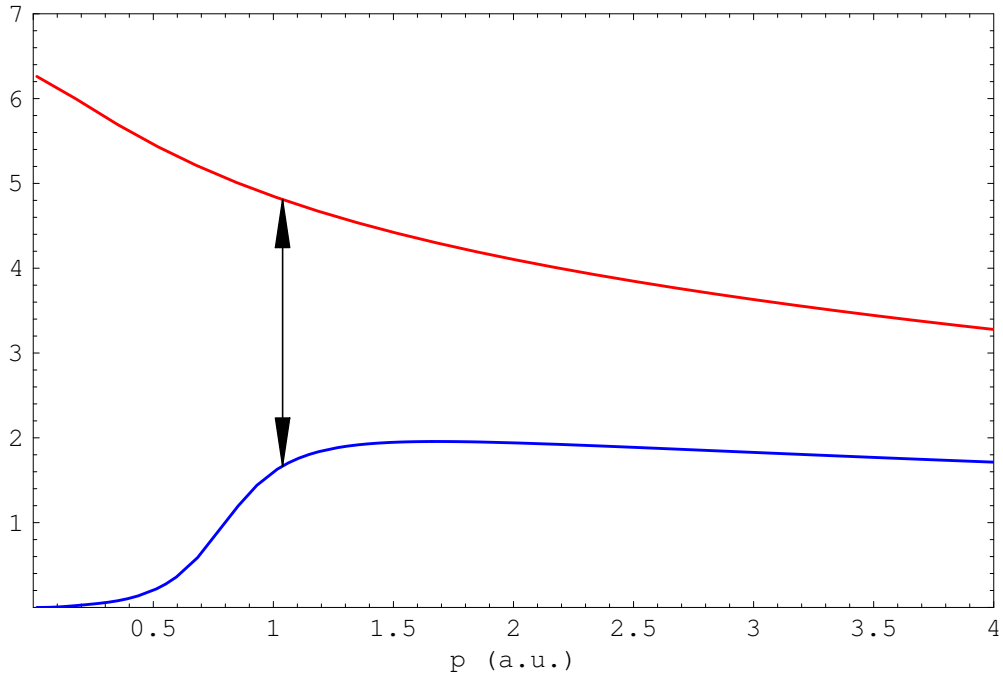

Figure 6. Phaseshifts for s- (upper curve) and p- (lower curve) waves for neutral Ne plotted against momentum $p = \sqrt{2T}$. The arrow denotes the place where the phaseshift difference equals π.

Here $[x]$ is the largest integer m less than x.

One may make further predictions concerning the number of diagonal crossings of trajectories if the sign of C in the expansion of the phaseshift for small momenta $p = \sqrt{2T}$ [37], is known:

$$\delta(p) \approx n\pi + Cp^{2\ell+1}. \tag{12}$$

Qualitatively, C is negative if the uppermost bound state of angular momentum ℓ is loosely bound, positive if it is tightly bound.

This allows us to predict that there is a diagonal crossing (and, hence, a trajectory of matrix element zero) for the $s \to p$ transition in the field of neutral Na, even though $n_s = 2$, and $n_p = 1$, so that the minimum number of the diagonal crossings from (8) is zero. The coefficients C for both the s - and p -waves in the field of Na are positive, so that both s and p phaseshifts increase with momentum (see Figure 7). However, the phaseshift of the s -wave grows faster with momentum, so that the difference between the s and p phaseshifts, $\delta_s(p) - \delta_p(p)$ grows at small momenta, starting from $(n_s - n_p)\pi = \pi$, becoming larger than π. The difference becomes zero in the limit of large momentum, therefore crossing π at some momentum (shown in Figure 7 by the arrow).

We note that for realistic atomic neutral potentials, the number of bound states with given angular momentum (i.e. the number of eigenvalues of the given momentum calculated in a frozen neutral potential), correlate with the number of atomic subshells with that momentum. This gives a possibility to connect directly the behavior of the trajectories of zeroes in bremsstrahlung and inverse bremsstrahlung processes to the

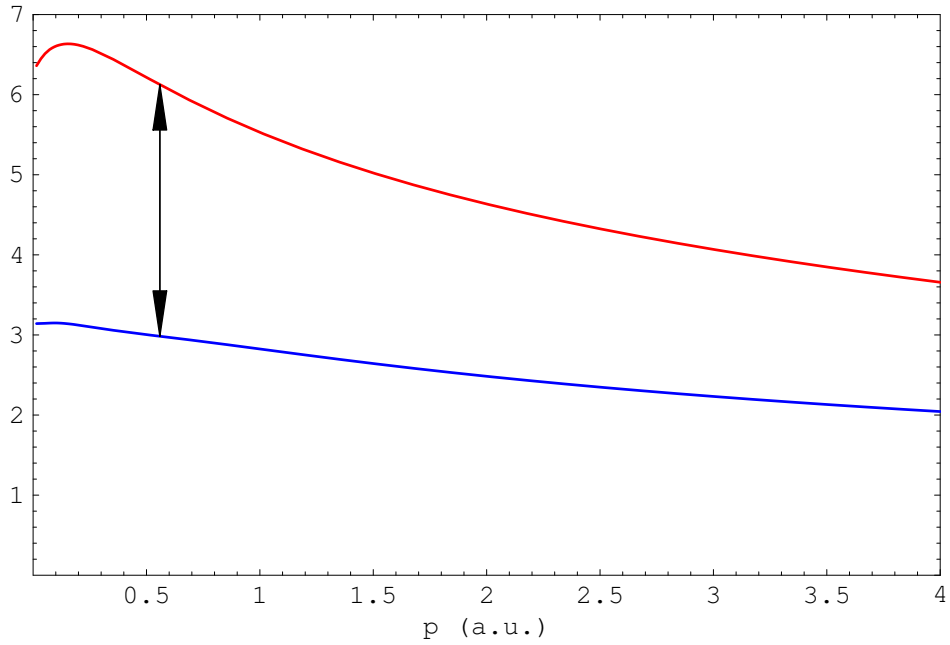

Figure 7. Same as in Figure 6 but for Na.

electronic configuration of the target atom.

4. Classical bremsstrahlung

It has long been established that the classical approach to bremsstrahlung calculations [2, 3] for low incident electron energies can produce useful results both in the point Coulomb case [38] and in the screened potentials [1, 5, 39]. In fact, the structures at low energies in bremsstrahlung were first noted classically in the energy dependence of the asymmetry parameter a_2 for several fixed ratios k/T [1]. Later the structures were also identified in the differential cross section $\omega \mathrm{d}\sigma/\mathrm{d}\omega$ [4]. Detailed analysis of these structures and comparison with the quantum case can be found in [5, 6, 39]

In the previous sections we showed that the quantum structures may be related to the zeroes of the radial matrix elements which occur for particular angular momenta at particular energies. In other words, in the quantum case the lack of contribution from some of the dominant radiative transitions (due to zeroes in corresponding matrix elements) results in the observed structures. In this section we describe a corresponding origin for the classical structures. We show that the classical structures have, essentially, the same origin as the quantum ones, namely, the lack of contribution from a certain range of angular momentum at certain incident electron energies.

In order to get a clear physical picture of the origin of the structures, we will take advantage of the fact, previously noted in section 2, that the structures are not sensitive to the ratio k/T, and they can be well characterized in the soft photon limit. In the soft photon limit the only parameter necessary for determining the singly and doubly differential cross sections is the electron scattering angle. Therefore, it turns out to

be possible to relate the structures to the behaviour of the scattering angle in certain ranges of angular momentum as incident energy changes.

We note the similarity between the classical and quantum cases. While the electron scattering angle θ is the single parameter which characterizes bremsstrahlung in the soft photon limit in the classical case, the scattering phase shift determines soft photon bremsstrahlung in the quantum case. The two quantities are both determined from the properties of the atomic potential, and they are connected (in WKB approximation) through the relation [40]

$$\frac{\theta(\ell)}{2} = \frac{\partial \delta_\ell^{\mathrm{WKB}}}{\partial \ell}. \tag{13}$$

4.1. Classical formalism in the soft photon limit

A formalism for classical bremsstrahlung and the soft-photon limit of dipole radiation is given in [3]. An extensive analysis of classical bremsstrahlung in screened atomic potentials, under the assumption that energy loss on trajectories is neglected, can be found in [1, 4, 39]. We do not reproduce these results here, rather we focus on the important points which help to understand the origin of the structures in the classical case.

The doubly differential cross section describing the radiation emitted into a solid angle $d\Omega_k$, in the frequency interval $(k, k + \mathrm{d}k)$, may be written in the same form as in the quantum case:

$$k\frac{\mathrm{d}^2\sigma}{\mathrm{d}\Omega_k \mathrm{d}k} = \frac{1}{4\pi} k\frac{\mathrm{d}\sigma}{\mathrm{d}k}\left[1 + \frac{a_2}{2} P_2(\cos\theta_k)\right]. \tag{14}$$

In the classical case the bremsstrahlung spectrum

$$k\frac{\mathrm{d}\sigma}{\mathrm{d}k} = \frac{8\pi}{3c^3}\,\mathcal{I}_1, \tag{15}$$

and the asymmetry parameter a_2,

$$a_2 = \frac{\mathcal{I}_2}{\mathcal{I}_1}, \tag{16}$$

are expressed in terms of quantities $\mathcal{I}_1$ and $\mathcal{I}_2$ which, in the soft photom limit, are simply given as quadrature integrals over the scattering angle $\Phi(E, \ell)$, considered as a function of angular momentum:

$$\mathcal{I}_1^{\mathrm{s-ph}}(T) = \frac{1}{\pi}\int_0^\infty [1 - \cos\Phi(T,\ell)]\,\ell\,\mathrm{d}\ell, \tag{17}$$

$$\mathcal{I}_2^{\mathrm{s-ph}}(T) = \frac{1}{2\pi}\int_0^\infty [1 - \cos\Phi(T,\ell)]\,[3\cos\Phi(T,\ell) - 1]\,\ell\,\mathrm{d}\ell, \tag{18}$$

$$\Phi(T,\ell) = \sqrt{\frac{2}{m}}\ell \int_{r_0(T,\ell)}^\infty \frac{\mathrm{d}r}{r^2\sqrt{T - V_{\mathrm{eff}}(r,\ell)}} - \pi. \tag{19}$$

Here

$$V_{\rm eff}(r,\ell) = V(r) + \frac{\ell^2}{2mr^2}, \tag{20}$$

$V(r)$ is the atomic potential, and $r_0(E,\ell)$ is the classical turning point defined by

$$E = V_{\rm eff}(r_0(E,\ell),\ell). \tag{21}$$

4.2. The origin of the structures in classical bremsstrahlung

The present discussion is based on [39], in which the structures in classical bremsstrahlung were examined in greater detail. Here, we briefly restate the main ideas, stressing the similarity between the classical and quantum descriptions.

Figure 8 illustrates the energy dependence of the classical bremsstrahlung cross section in the soft photon limit. For comparison, the quantum result for $k/T = 0.01$ is reproduced from Figure 1. The corresponding energy dependence of the asymmetry parameter is shown in Figure 9. The quantum and classical cross sections and asymmetry parameters agree well at higher electron energies. At lower energies both quantum and classical results exhibit structures, although their quantitative agreement gets worse.

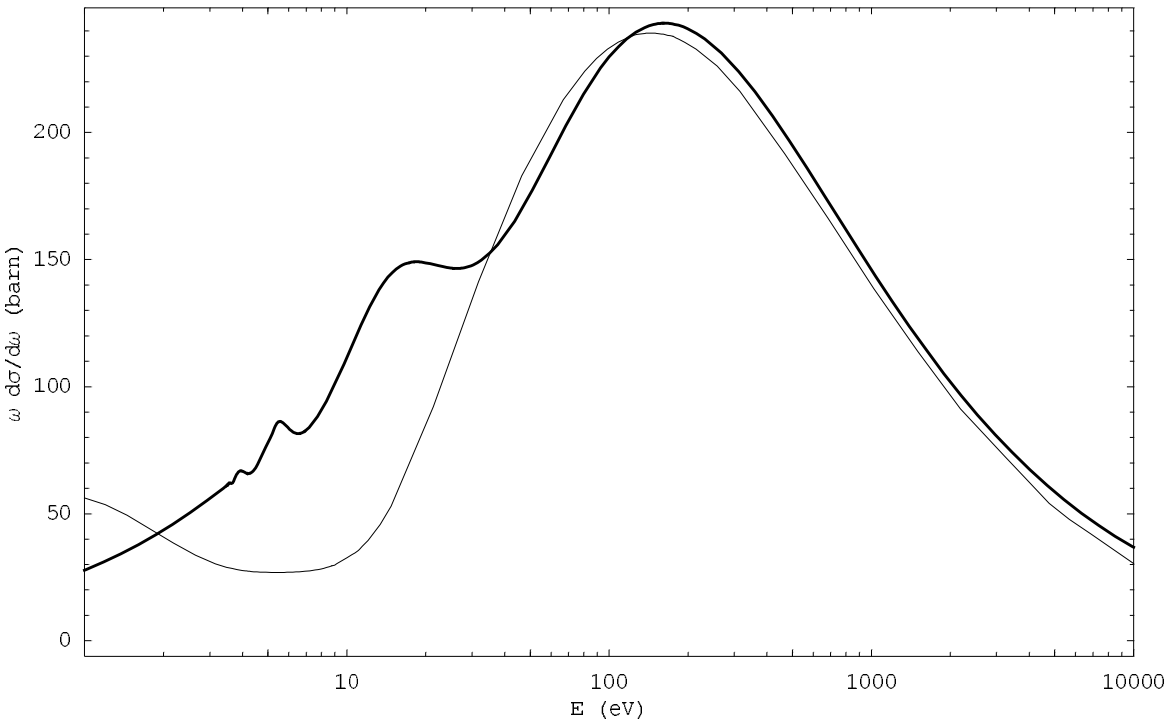

Figure 8. Energy dependence of the classical (thick line) and quantum (thin line) bremsstrahlung cross section in the soft-photon limit, for Al in a Hartree-Fock potential. The figure is taken from [6].

What are the origins of the structures in the classical case? To answer this question consider the integrand in (17),

$$J_1(E,\ell) \equiv \ell\,[1 - \cos\Phi(T,\ell)]\,, \tag{22}$$

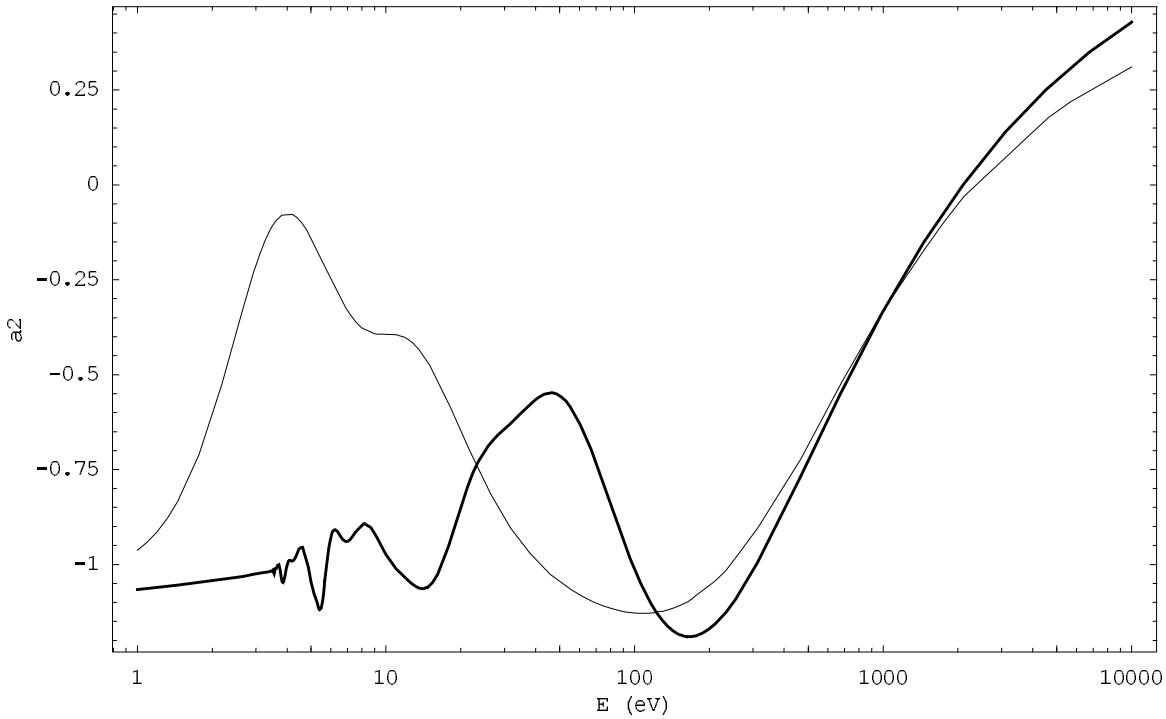

Figure 9. Energy dependence of the classical (thick line) and quantum (thin line) asymmetry parameter a_2 in the soft-photon limit, for Al in a Hartree-Fock potential. The figure is taken from [6].

plotted in Figures 10 and 11, which vanishes every time the scattering angle $\Phi(T,\ell)$ (shown in the insets) as a function of ℓ crosses $2n\pi$. Such zeroes in (22) at particular ℓ, which occur over broad ranges in T, are not directly connected to the minima in the cross section. However, if $\Phi(T,\ell) \simeq 2n\pi$ in a wider range of ℓ, this can lead to a minimum in the cross section. This can happen, for instance, when $\Phi(T,\ell)$ has a broad maximum near $2n\pi$, see, e.g., $T = 26$ eV in Figure 10. Another possibility is a "shoulder" on a wing of the maximum, such as occurs in Al for $E \approx 6.5$ eV (Figure 11). The former situation gives rise to the first minimum in the cross section, while the latter situation gives the second minimum (moving from larger to smaller energies). Analogously, a maximum of the cross section occurs when the scattering angle is approximately $(2n+1)\pi$ in a wider region of ℓ.

The regions of ℓ in which the scattering angle stays around $2n\pi$ or $2(n+1)\pi$ levels provide suppressed or enhanced contributions, respectively, to the total value of the integral. In order to get a semi-quantitative estimate for these contributions we divide the interval of integration into three subintervals in such a way that the second subinterval contains the region where the scattering angle stays around $2n\pi$ or $2(n+1)\pi$ levels. The results of integration over the three subintervals are shown as histograms in Figures 10 and 11. The darker bars correspond to the energies for which minimuma of the cross section are observed. The lighter bars correspond to the energies for which maxima neighbouring to the minima are observed. It can be seen that the contribution

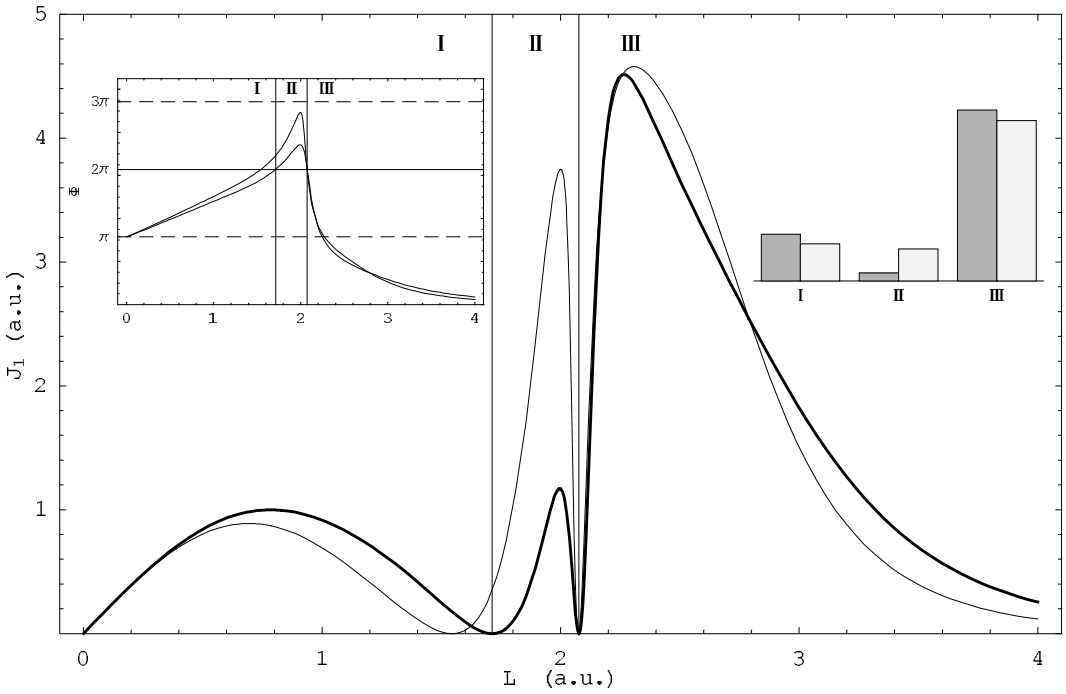

Figure 10. The subintegral expression J_1 (22) for Al as a function of ℓ for two energies, corresponding to the first minimum (thick line, $E = 26$ eV) and maximum (thin line, $E = 19$ eV) of the cross section. In the inset we give the scattering angle $\Phi(E, \ell)$ as a function of ℓ for these two energies (again, the thick line corresponds to the minimum, the thin line to the maximum). We introduce three intervals in ℓ: I – $\ell \in (0, \ell_{\rm I})$, II – $\ell \in (\ell_{\rm I}, \ell_{\rm II})$, and III – $\ell \in (\ell_{\rm II}, \infty)$. $\ell_{\rm I}$ and $\ell_{\rm II}$ are the solutions of $\Phi(E, \ell) = 2\pi$ for $E = 26$ eV. The result of integration over these three regions is given in the histogram (darker bars correspond to the minimum, $E = 26$ eV). The figure is taken from [39].

to the total integral from the region II is depressed for the minima and is somewhat enhanced for the maxima. In fact, this is a general type of behavior which is repeated for every pair of minimum/maximum (26 eV and 19 eV, 6.5 eV and 5.5 eV, and so forth). We observe such behavior whenever there are structures in the cross section.

Therefore, the origin of the structures in the classical case is essentially the same as in the quantum case. It is the lack of contributions from some values (regions) of angular momenta at certain incident electron enegies. The only difference is that in the quantum case the cross section is a sum over discrete angular momentum contributions while in the classical case the cross section is obtained by integration over the continuous range of angular momenta.

Another similarity to the quantum case is that the structures are not possible in the point Coulomb field. The screened nature of atomic potential is crucial for observing the structures. Indeed, for the first minimum to occur the scattering angle must increase from its starting value of π at zero angular momenta to the level of 2π. This is not possible for the point Coulomb potentials, for which the scattering angle is a monotonous decreasing function of angular momentum. In the screened case it is also true for high electron energies. However, at some energy (typically, it is several hundred eVs) the

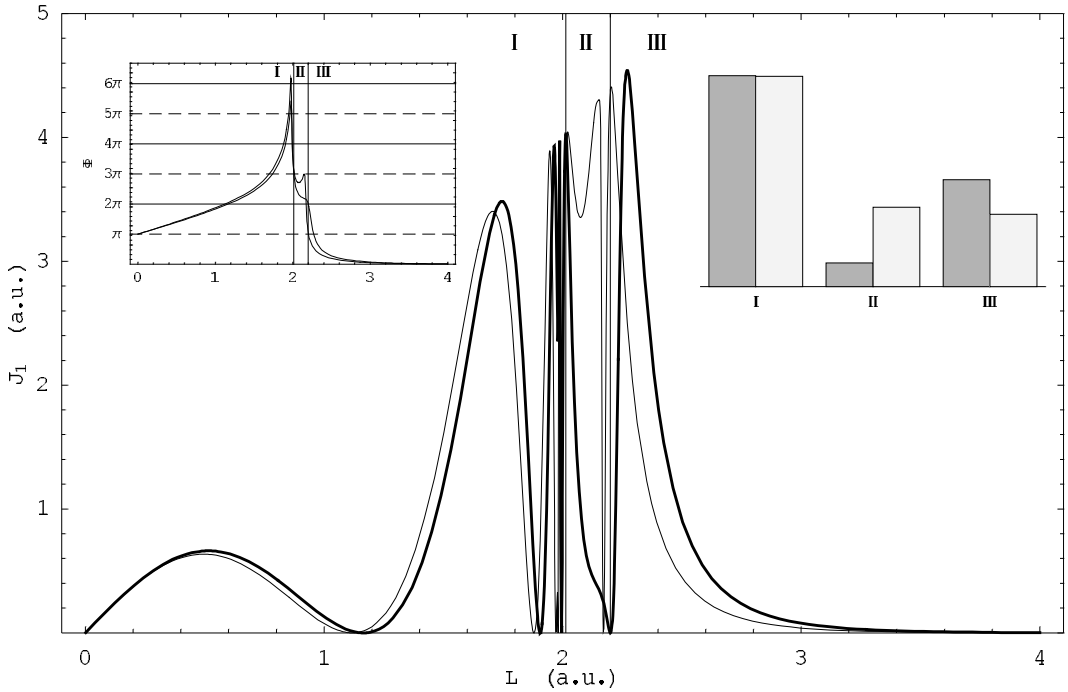

Figure 11. Same as in the Figure 10, but for energies corresponding to the second minimum (thick line, $E = 6.5$ eV) and maximum (thin line, $E = 5.5$ eV) of the cross section. $\ell_{\rm I}$ and $\ell_{\rm II}$ are defined here by the following equations: $\Phi(E, \ell_{\rm I}) = 3\pi$ and $\Phi(E, \ell_{\rm II}) = 2\pi$ for $E = 6.5$ eV. The figure is taken from [39].

behaviour of the scattering angle at small angular momenta changes, and the scattering angle increases at small ℓ. At large ℓ it diminishes to zero which implies that there is a maximum of the scattering angle at some value of ℓ. This smooth wide maximum is connected to two internally connected physical phenomena.

The first one is the main maximum in the energy dependence of the bremsstrahlung cross section ($T = 170$ eV in Figure 8). In fact, this maximum has the same origin as the set of smaller ones: an enhanced contribution from some range of angular momentum. Indeed, for some energy interval the scattering angle has a wide smooth low maximum, staying around π in a broad interval of angular momentum, so that $1 - \cos\Phi \approx 2$. This leads to large values of the integral for these energies and a high prominent maximum in the cross section. For these same energies, another phenomenon is observed in elastic electron scattering. Namely, a scattering angle staying around π in a broad interval of angular momentum corresponds to enhanced backward scattering; this phenomen in elastic electron scattering is called Coulomb glory [41, 42]. It appears that a similar argument has been used recently by Zon [43] in explaining experiments on bremsstrahlung from electrons of intermediate energies.

The fact that the scattering angle for certain electron energies can stay around $n\pi$ in a broader interval of angular momentum is sufficient for explanation of the structures

seen in low energy classical bremsstrahlung. We will not discuss other features observed in the behaviour of the scattering angle as the electron energy changes. We refer to the original paper [39], where all these effects and their contribution to the overall behaviour of the scattering angle are considered in detail.

Acknowledgements

The authors are grateful to Drs. A. V. Korol and D. B. Uskov for fruitful discussions. Partial financial support from NSF Grant 0201595, NSF/NATO Grant 0209594, RFBR Grant 03-02-16415a, and INTAS grant 03-51-6170 is also acknowledged.

References

[1] Kim, L., Pratt, R. H., 1987. Numerical calculation of classical bremsstrahlung. Phys. Rev. A 36, 45-58.

[2] Jackson, J. D., 1975. Classical electrodynamics. John Wiley and Sons, New York.

[3] Landau, L. D., Lifshitz, E. M., 1959. The classical theory of fields. Addison-Wesley, Reading, Massachusetts.

[4] Shaffer, C. D., 1996. PhD thesis. University of Pittsburgh, Pittsburgh, PA.

[5] Florescu, A., Obolensky, O. I., Shaffer, C. D., Pratt R. H., 2001. Structures in the energy dependence of classical and quantum bremsstrahlung. In: Application of accelerators in research and industry, eds. Duggan, J. L. and Morgan, I. L., p. 60-53, Sixteenth international conference, Denton, Texas 2000. AIP Conference Proceedings 576, Melville, New York.

[6] Uskov, D. B., Pratt, R. H., Korol, A. V.,Obolensky, O. I., 2003. Comparison of classical and quantum bremsstrahlung. In: Application of accelerators in research and industry, eds. Duggan, J. L. and Morgan, I. L., p. 119-123, Seventeenth international conference, Denton, Texas 2002. AIP Conference Proceedings 680, Melville, New York.

[7] Gnatchenko, E. V., Tkachenko, A. A., Verkhovtseva, E. T., 2002. The bremsstrahlung induced by 0.3-2 keV electron scattering by Ar atoms. Optics and Spectroscopy 92, 13-16.

[8] Gnatchenko, E. V., Tkachenko, A. A., Verkhovtseva, E. T., 2002. Specific features of ultrasoft X-ray bremsstrahlung on scattering of intermediate energy electrons by Argon atoms. Surf. Rev. Lett. 9, 651-654.

[9] LaJohn, L. A., Pratt, R. H., 2003. Relativistic electric-dipole matrix-element zeros. Phys. Rev. A 67, 032701 (6 pp.).

[10] Manson, S. T., 1985. Systematics of zeroes in dipole matrix elements for photoionizing transitions: Nonrelativistic calculations. Phys. Rev. A 31, 3698-3703.

[11] Msezane, A. Z., Manson, S. T., 1982. Generality and systematics of multiple minima in photoionization cross sections of excited atoms. Phys. Rev. Lett. 48, 473-475.

[12] Yin, R. Y., Pratt, R. H., 1987. Survey of relativistic Cooper minima. Phys. Rev. A 35, 1149-1153.

[13] Yin, R. Y., Pratt, R. H., 1987. Ionic and point Coulomb relativistic Cooper minima. Phys. Rev. A 35, 1154-1158.

[14] Amusia, M. Ya., Pratt, R. H., 1992. Emission and absorption of radiation by structured particles. Comments on Atomic and Molecular Physics 28, 247-258.

[15] Pratt, R. H., Feng, I. J., 1985. Electron-atom bremsstrahlung. In: Atomic Inner-Shell Physics, edited by B. Crasemann, Chapter 12, p. 533-580, Plenum, New York, and references therein.

[16] Tsytovich, V. N. and Ojringel, I. M. (editors), 1993. Polarizational bremsstrahlung. Plenum, New York.

[17] Korol, A. V., Solov'yov, A. V., 1997. Polarizational bremsstrahlung of electrons in collisions with atoms and clusters. J. Phys. B 30, 1105-1150.

[18] Korol, A. V., Solov'yov, A. V. Polarizational bremsstrahlung in non-relativistic collisions, In: This issue.
[19] Kogan, V. I., Kukushkin, A. B., Lisitsa, V. S., 1992. Kramers electrodynamics and electron-atomic radiative-collisional processes. Phys. Rep. 213, 1-116.
[20] Astapenko, V. A., Bureeva, L. A., Lisitsa, V. S., 2000. Classical and quantum theories of the polarization bremsstrahlung in the local electron density model. JETP 90, 434-446.
[21] Obolensky, O. I., Korol, A. V., Pratt, R. H., 2003. Unpublished.
[22] Sobelman, I. I., 1979. Atomic spectra and radiative transitions. Springer, Berlin.
[23] Tseng, H. K., Pratt, R. H., 1971. Exact screened calculations of atomic field bremsstrahlung. Phys. Rev. A 3, 100-115.
[24] Zhdanov, V. P., 1978. Fizika Plazmi 4, 128-133 (in Russian).
[25] Tseng, H. K., 1989. Nonrelativistic calculation of elementary process of electron bremsstrahlung from atoms. Phys. Rev. A 40, 6826-6830.
[26] Veniard, V., Piraux, B., 1990. Continuum-continuum dipole transitions in femtosecond-laser-pulse excitation of atomic hydrogen. Phys. Rev. A 41, 4019-3034.
[27] Korol, A. V., 1993. Singularities in the free-free dipole matrix element. J. Phys. B 26, 4769-4775.
[28] Korol, A. V., 1994. General formula for the singular part of the free-free dipole matrix element. J. Phys. B 27, L103-L107.
[29] Uskov, D. B., Pratt, R. H., 2003. Unpublished.
[30] Obolensky, O. I., Korol, A. V., Pratt, R.H., 2004. Trajectories of matrix element zeroes. Rad. Phys. Chem. 71, 677-678.
[31] Oh, Sung Dahm, Pratt, R. H., 1986. Nonvanishing of allowed Coulomb dipole matrix elements. Phys. Rev A 34, 2486-2487.
[32] Oh, Sung Dahm, Pratt, R. H., 1992. Positiveness and monotonicity of free-free Coulomb dipole matrix elements. Phys. Rev A 45, 1583-1586.
[33] Low, F. E., 1958. Bremsstrahlung of very low-energy quanta in elementary particle collisions. Phys. Rev. 110, 974-977.
[34] Newton, R. G., 1982. Scattering theory of waves and particles. Springer, New York.
[35] Iwinski, Z. R., Rosenberg, L., Spruch, L., 1985. Nodal structure of zero-energy wave functions: New approach to Levinson's theorem. Phys. Rev. A 31, 1229-1240.
[36] Rosenberg, L., 1995. Levinson-Seaton theorem for potentials with an attractive Coulomb tail. Phys. Rev. A 52, 3824-3826.
[37] Mott, N. F., Massey, H. S. W., 1987. The theory of atomic collisions. Clarendon Press, Oxford.
[38] Florescu, V., Steiner, V., Burlacu, L., 1987. New analytic forms for the classical bremsstrahlung angular distributions in the Coulomb case. J. Phys. B 20, 427-442.
[39] Florescu, A., Obolensky, O. I., Pratt, R. H., 2002. Structures in low-energy classical bremsstrahlung. J. Phys. B 35, 2911-2926.
[40] Bransden, B. H., McDowell, M. R. C., 1992. Charge exchange and the theory of ion-atom collisions. Clarendon Press, Oxford. p. 28.
[41] Demkov, Yu. N., Ostrovsky, V., N., Telnov, D. A., 1984. Zh. Eksp. Teor. Fiz. 84, 442-450 (in Russian). (English translation: 1984. Sov. Phys. – JETP 59, 257-261.)
[42] Demkov, Yu. N., Ostrovsky, V., N., Telnov, D. A., 2001. Enhanced backscattering in antiproton-atom collision: Coulomb glory. J. Phys. B 34, L595-L600.
[43] Zon, B.A., 2004. Private communication.